JACS
JOURNAL OF THE AMERICAN CHEMICAL SOCIETY
pubs.acs.org/JACS
Article

Control of Molecular Bonding Strength on Metal Catalysts with Organic Monolayers for CO_2 Reduction

Jing Zhang, Shyam Deo, Michael J. Janik, and J. Will Medlin*

Cite This: J. Am. Chem. Soc. 2020, 142, 5184−5193
Read Online

ABSTRACT: The development of separate levers for controlling the bonding strength of different reactive species on catalyst surfaces is challenging but essential for the design of highly active and selective catalysts. For example, during CO_2 reduction, production of CO often requires balancing a trade-off between the adsorption strength of the reactant and product states: weak binding of CO is desirable from a selectivity perspective, but weak binding of CO_2 leads to low activity. Here, we demonstrate a new method of controlling both CO_2 adsorption and CO desorption over supported metal catalysts by employing a single self-assembly step where organic monolayer films were deposited on the catalyst support. Binding of phosphonic acid monolayers on supported Pt and Pd catalysts weakened CO binding via a through-support effect. The weakened CO adsorption was generally accompanied by decreased adsorption and reactivity of CO_2. However, by the incorporation of basic amine functions at controlled positions in the modifying film, strong CO_2 adsorption and hydrogenation reactivity could be restored. Thus, both through-surface and through-space interactions could be manipulated by design of the organic modifiers. After surface modification, the catalysts exhibited significantly improved selectivity (up to ~99% at conversions near 50%) and activity toward CO production. Moreover, the rate of deactivation was notably reduced due to prevention of CO poisoning.

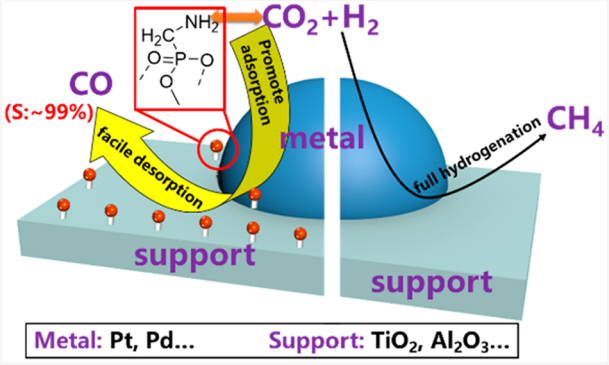

INTRODUCTION

Reactions occurring on a catalytic surface require a balance between strong enough binding to enable the adsorption and activation of reactant species but weak enough binding to allow rapid desorption of products. Many important reactions require a control of binding strength of multiple reactive species on the catalyst surface.[1] For example, the catalytic conversion of CO_2 through the reverse water−gas shift (RWGS) reaction to produce CO, which is an important feedstock for many significant industrial processes (such as the Fischer−Tropsch synthesis), is a promising route to reduce CO_2 emissions and replace fossil fuels in terms of a sustainable carbon cycle.[2−7]

For the atmospheric-pressure RWGS conversion of CO_2, the most widely accepted mechanism consists of adsorption and activation of CO_2 at the metal/oxide interface of supported metal catalysts. These steps are followed by hydrogenation and/or dissociation to form chemically adsorbed CO, which can either undergo desorption to form the desired product or further hydrogenation to form CH_4.[8−10] The active and selective catalyst for RWGS should be capable of adsorbing/activating CO_2, dissociating hydrogen, and allowing for CO desorption.[11] The simultaneous control of binding strength of these key surface species, however, is extremely challenging. Industrial RWGS catalysts, such as ZnO/Al_2O_3 and ZnO/Cr_2O_3, typically require high operating temperatures at or above 600 °C to facilitate CO_2 activation and selective CO production,[12] resulting in severe deactivation and energy cost.[13,14] To efficiently produce CO at milder conditions, various strategies have been used to prepare multifunctional catalysts[12,15−23] and/or control the size of the supported small metal clusters[24−26] even down to atomic dispersions.[27,28] In many cases, these approaches require complex or costly catalyst synthesis steps.

Here, we demonstrate a new mechanism for simultaneously tuning binding strengths of multiple reactive species at the interface of supported metal catalysts for efficient and selective production of CO from CO_2. In this method, organic ligands were assembled on the support to control the surface environment at the interface. The key to this strategy was to take advantage of the versatility in design of the ligands, which can moderate catalytic reactions both by surface electronic

Received: December 2, 2019
Published: February 21, 2020

https://dx.doi.org/10.1021/jacs.9b12980
J. Am. Chem. Soc. 2020, 142, 5184−5193

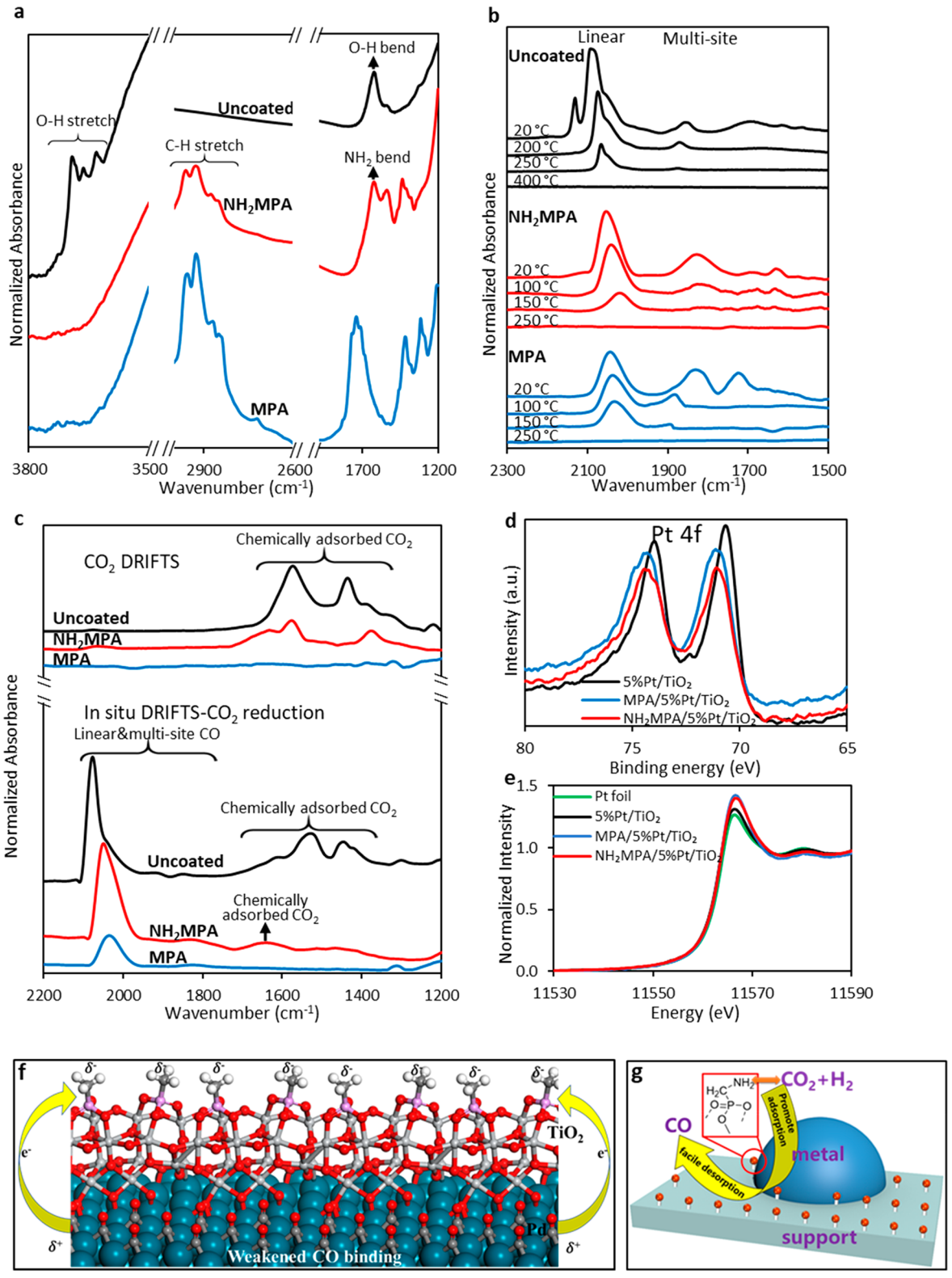

Figure 1. Characterization of catalyst materials. (a) FTIR spectra for 5%Pt/TiO_2 before and after PA deposition. (b) DRIFT spectra of CO adsorbed on 5%Pt/TiO_2 and PA-treated 5%Pt/TiO_2 following thermal treatment at elevated temperatures. (c) DRIFT spectra of CO_2 adsorbed on 5%Pt/TiO_2 and PA treated 5%Pt/TiO_2 at 20 °C and *in situ* CO_2 reduction conditions at 250 °C. (d) XPS analysis of 5%Pt/TiO_2 and PA treated 5%Pt/TiO_2. (e) Pt L_3-edge XANES spectra of Pt foil, 5%Pt/TiO_2, and PA treated 5%Pt/TiO_2. (f) DFT model of a TiO_2/Pd interface. MPA phosphonate ligands are bound to TiO_2, and CO is bound at high coverage to Pd near the interface. Note that only one (tridentate) of multiple possible binding configurations is shown. (g) Proposed scheme showing how the functional groups in phosphonate ligands promoted adsorption of CO_2 and desorption of CO.

https://dx.doi.org/10.1021/jacs.9b12980
J. Am. Chem. Soc. 2020, 142, 5184−5193

effects and via noncovalent interactions near the active site.[29] In this case, the ligand phosphonate binding group induced a desired weakening of CO binding to the metal but at the cost of lowering the rate of activation of the CO_2 reactant at the metal−support interface. However, the activity could be restored by tuning the chemistry of the ligand to favor specific, stabilizing interactions with CO_2. A simple self-assembly process was found to be applicable to different types of metals and supports, significantly improving selectivity and activity toward CO production over the supported metal catalysts while limiting the rate of deactivation. As a result, traditional supported metal catalysts could be readily transformed into active, selective, and stable RWGS catalysts.

RESULTS

Characterization. A 5%Pt/TiO_2 catalyst prepared by incipient wetness impregnation was modified by monolayers of different phosphonic acids (PA). As indicated by inductively coupled plasma (ICP) and X-ray photoelectron spectroscopy (XPS) analysis (Figure S1 and Tables S1 and S2 in the Supporting Information), PAs were deposited at high surface densities on the catalyst. Furthermore, we measured Fourier transform infrared (FTIR) spectra for long-chain PAs (Figure S2 in the Supporting Information) and observed an asymmetric methylene stretching peak (~2,920 cm^{-1}) consistent with relatively well-ordered alkyl domains on the surface.[30,31] FTIR spectra (Figure 1a) for catalysts functionalized with shorter-chain methyl phosphonic acid (MPA) and aminomethyl phosphonic acid (NH_2MPA) also led to the appearance of C−H stretching vibration peaks. It was found that the unmodified 5%Pt/TiO_2 exhibited O−H stretching (~3600−3700 cm^{-1}) and O−H bending (~1630 cm^{-1}) modes that were attributed to surface hydroxyl groups.[32] After the deposition, peaks associated with the O−H stretch disappeared, which can be explained by the generally agreed mechanism for PA deposition on metal oxides: the PAs undergo a condensation reaction with the surface hydroxyl species to bind on the surface, resulting in consumption of hydroxyl groups.[33,34] Therefore, the peak at ~1630 cm^{-1} after NH_2MPA deposition could be assigned to NH_2 bending.[35] This was confirmed by comparing the spectra in Figure 1a and Figure S2 in the Supporting Information, which shows that only the catalysts modified with amine-containing PAs have the peak at around 1630 cm^{-1}. Therefore, the amine functionality on the PA tail was retained in the organic monolayers.

PA modification of Pt/TiO_2 was found to strongly decrease the adsorption strength of CO on the surface. The temperature-programmed desorption (TPD) of CO measured via diffuse reflectance infrared Fourier transform spectroscopy (DRIFTS) (Figure 1b) showed the temperature for complete CO desorption decreased from 400 to 250 °C after PA modification. Because CO binding is expected to occur on Pt sites, we hypothesized that PA modification led to electronic perturbation of Pt. Consistent with this hypothesis, XPS analysis (Figure 1d) showed a ~0.5 eV shift toward higher binding energy for Pt 4f after the modification. Generally, the Pt 4f binding energy is ~1.4 eV higher for PtO than metallic Pt; therefore, the XPS analysis suggests a partial charge transfer from Pt to the substrate.[36,37] Moreover, Pt X-ray absorption near edge spectroscopy (XANES) (Figure 1e) showed relatively greater white line intensity for PA-modified 5%Pt/TiO_2, indicating some degree of Pt oxidation.[38] Consistent with the XPS results, the Pt still appears to remain in the metallic state since there is no obvious change in the shape of the XANE spectra. This modification of electronic properties would be expected to lead to a reduction in metal's ability to coordinate CO through backdonation of electrons into 2 π orbitals, resulting in a weaker metal-CO bond.[39] Since the PA can only covalently bind to the oxide support instead of Pt,[40] it was speculated that the charge transfer is induced by change of electronic properties of the TiO_2 upon the PA deposition, where the condensation between PA's head groups (P−OH) and the surface hydroxyl groups effectively replaced the H on TiO_2 with the more electron-withdrawing phosphonate group.[41] Similar shifts of Pt 4f binding energy in the PA-modified catalysts were also observed after exposure to high-temperature reducing conditions similar to those used for CO_2 hydrogenation (Figure S3). The similar degree of binding energy shift (Figure 1d) and similarly lower desorption temperature of CO (Figure S4) among catalysts modified by different PA ligands further suggests that the PA headgroup on the substrate (rather than the organic tail functionalities) was responsible for the observed effects.

To the best of our knowledge, the use of ligands on a support to control electonic properties of metal nanoparticles has not previously been reported. To gain additional insights into the mechanism, we carried out density functional theory (DFT) calculations by employing a previously described interface model consisting of TiO_2 nanowires deposited over a Pd(111) surface[42] to examine how PA coadsorption altered the binding strength of CO near the interface. For simplicity, MPA was chosen as a representative PA in the calculation. Several different binding modes have been reported to be present in PA monolayers on TiO_2.[43] Therefore, during the calculation we considered monodentate, bidentate, and tridentate adsorption modes, corresponding to stoichiometric MPA adsorption on TiO_2 (MPA), MPA adsorption with dehydrogenation (MPA-2H), and MPA adsorption with dehydration via deprotonation and removal of a surface O atom (MPA-H_2O), respectively (Figure S5). Bader charge analysis indicated electrons were transferred from Pd to MPA for all the three adsorption modes (SI Tables S3−S5). At high or medium MPA coverage, both "MPA-2H" and "MPA" adsorption modes had significant effects on the CO adsorption energy, weakening it by up to 0.39 eV, while the "MPA-H_2O" mode had a minimal effect on the CO adsorption energy (SI Tables S3−S5). Given the coexistence of multiple binding modes in PA monolayers on TiO_2, an overall effect of CO destabilization would be expected to result from the MPA modification. Consistent with experimental results, the DFT results suggested the weakened CO-metal binding after MPA adsorption on TiO_2 was due to electron transfer from the metal to the phosponate anions. A conceptual picture of how the MPA binding to TiO_2 affects electronic properties and CO adsorption near the TiO_2/Pd interface is illustrated in Figure 1f. The detailed DFT examination of MPA modifier effects on CO binding strength is described in the Supporting Information.

PA modification of Pt/TiO_2 also strongly influenced the binding of CO_2. It has been shown that metal alone cannot effectively catalyze CO_2 hydrogenation due to weak CO_2 binding on metal.[10] Therefore, oxide supports were used to facilitate the reaction via increased CO_2 binding, where reducible metal-oxide support (such as TiO_2, CeO_2, etc.) outperformed irreducible supports (SiO_2, Al_2O_3, etc.) in terms

https://dx.doi.org/10.1021/jacs.9b12980
J. Am. Chem. Soc. 2020, 142, 5184−5193

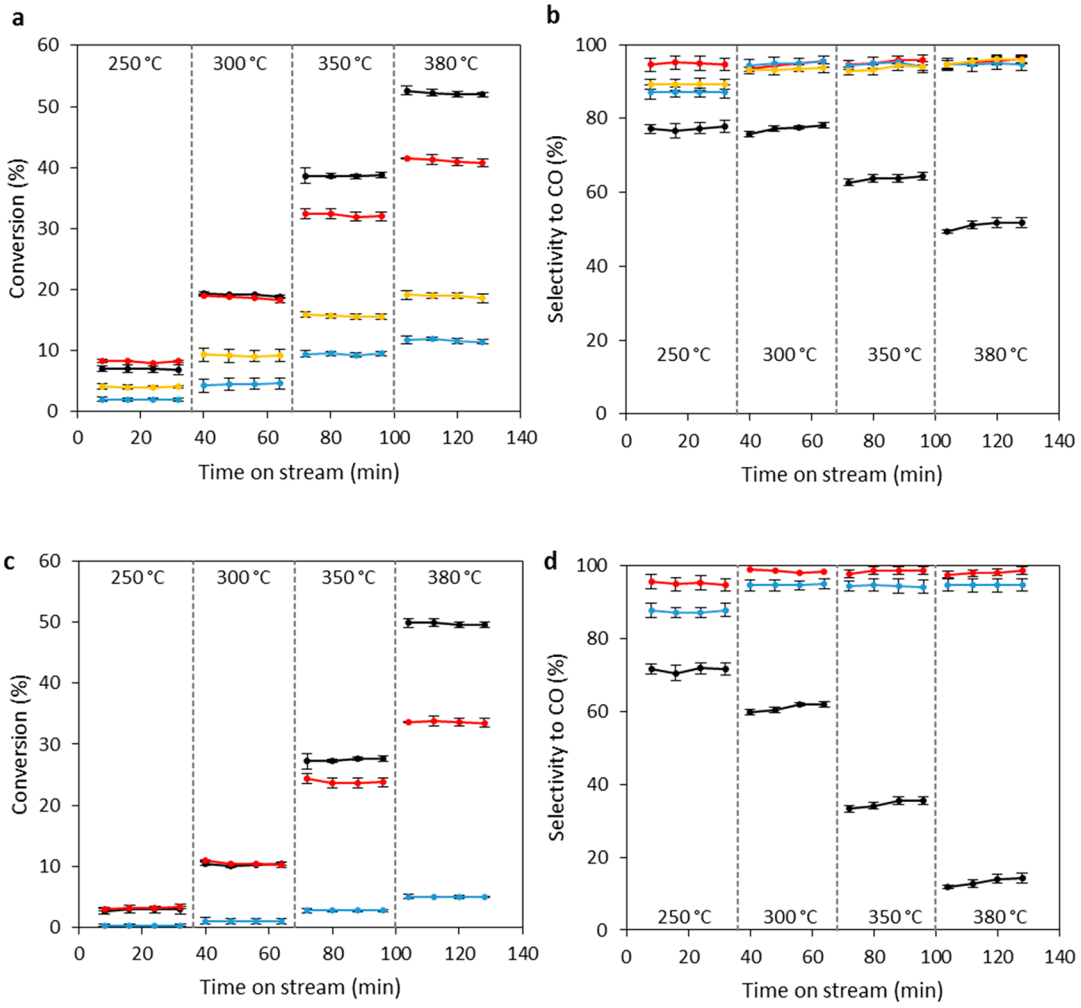

Figure 2. CO_2 reduction using 5%Pt/TiO_2 (a,b) and 5%Pd/TiO_2 (c,d) before and after being treated by PA. (Parts a and c) CO_2 conversion and (parts b and d) CO selectivity with time on stream at different temperatures. For parts a and b, black: 5%Pt/TiO_2; red: NH_2MPA/5%Pt/TiO_2; yellow: BZPA/5%Pt/TiO_2; blue MPA/5%Pt/TiO_2; catalyst loadings were kept at 80 mg for each case. For parts c and d, black: 5%Pd/TiO_2; red: 5%Pd@NH_2MPA/TiO_2; blue: NH_2MPA/5%Pd/TiO_2; catalyst loadings were kept at 140 mg for each case. Error bars indicate s.d. of triplicate runs.

of the activity.[3,10] CO_2 DRIFT spectra (Figure 1c) for the unmodified 5%Pt/TiO_2 at 20 °C and *in situ* reaction conditions showed chemically adsorbed CO_2 in the form of bicarbonate and carbonate species.[44,45] In contrast, MPA-treated Pt/TiO_2 did not show any characteristic peaks for chemically adsorbed CO_2, which was probably caused by the elimination of OH groups during PA deposition.[5,46] However, the NH_2MPA-treated 5%Pt/TiO_2 showed chemically adsorbed CO_2 both at 20 °C and *in situ* reaction conditions, with DRIFTS peaks at frequencies that have been assigned to carbamate and NH_3^+ deformation modes from CO_2 adsorption onto NH_2 sites.[35,47] The promotion effect of the amine toward CO_2 adsorption also applied to longer-chain PAs, such as 3-aminopropylphosphonic acid (3-NH_2PPA) (Figure S6). In addition, the adsorption of CO_2 did not require the presence of metal (Figure S7). These results indicate that although PA deposition consumes surface hydroxyl groups that favor CO_2 adsorption, incorporation of the amine group in PAs can restore the capability to bind CO_2 through an acid−base interaction. A conceptual depiction of how the PA ligands on supported metal catalyst affect CO and CO_2 interactions with the surface is illustrated in Figure 1g.

CO_2 Hydrogenation. Catalysts were evaluated for atmospheric-pressure CO_2 hydrogenation at a temperature range from 250 to 380 °C, conditions for which CO and CH_4 are typically observed as the major products.[27] Figure 2b shows that the modification of 5%Pt/TiO_2 with PAs significantly improved the selectivity toward CO up to ∼95% over almost the entire reaction temperature range, even at high CO_2 conversions (for NH_2MPA/5%Pt/TiO_2 at 380 °C). Since CH_4 has been shown to be produced in a series reaction from CO,[8−11] this suggests the produced CO could not undergo further hydrogenation to form CH_4. It should be noted that the PA ligands were stable under the reaction conditions (Figure S8). The degree of selectivity promotion (Figure 2b) was similar among different PAs, consistent with the similar CO desorption temperatures for all PA-modified 5%Pt/TiO_2 samples (Figure S4). Figure 2a showed much lower conversion for MPA and benzylphosphonic acid (BZPA) modified 5%Pt/TiO_2 compared with the unmodified 5%Pt/TiO_2 when equal amounts of catalyst were used. This loss in activity was attributed to a loss of binding sites for CO_2 at the metal−support interface where the adsorbed CO_2 can be readily hydrogenated by spillover H atoms provided by the metal.

https://dx.doi.org/10.1021/jacs.9b12980
J. Am. Chem. Soc. 2020, 142, 5184−5193

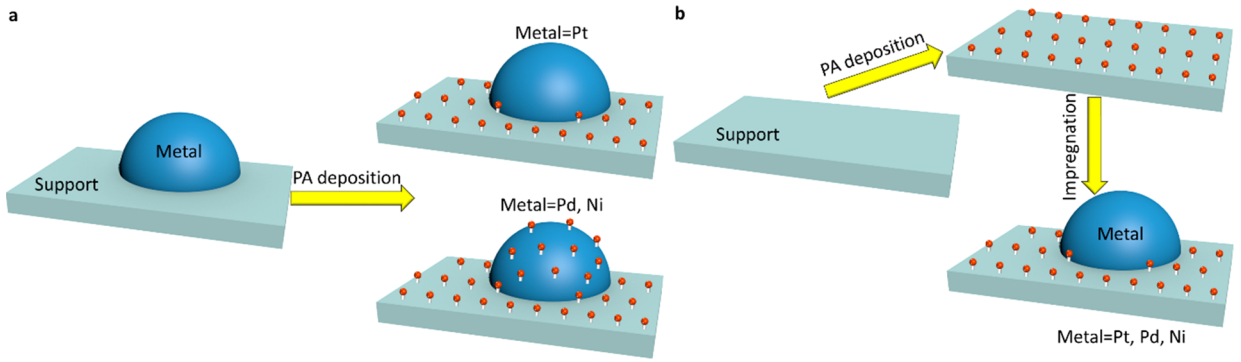

Figure 3. Schemes showing (a) phosphonic acid deposition on a supported metal catalyst, (b) phosphonic acid deposition on a catalyst support followed by introduction of metal through incipient wetness impregnation (referred as "reverse deposition").

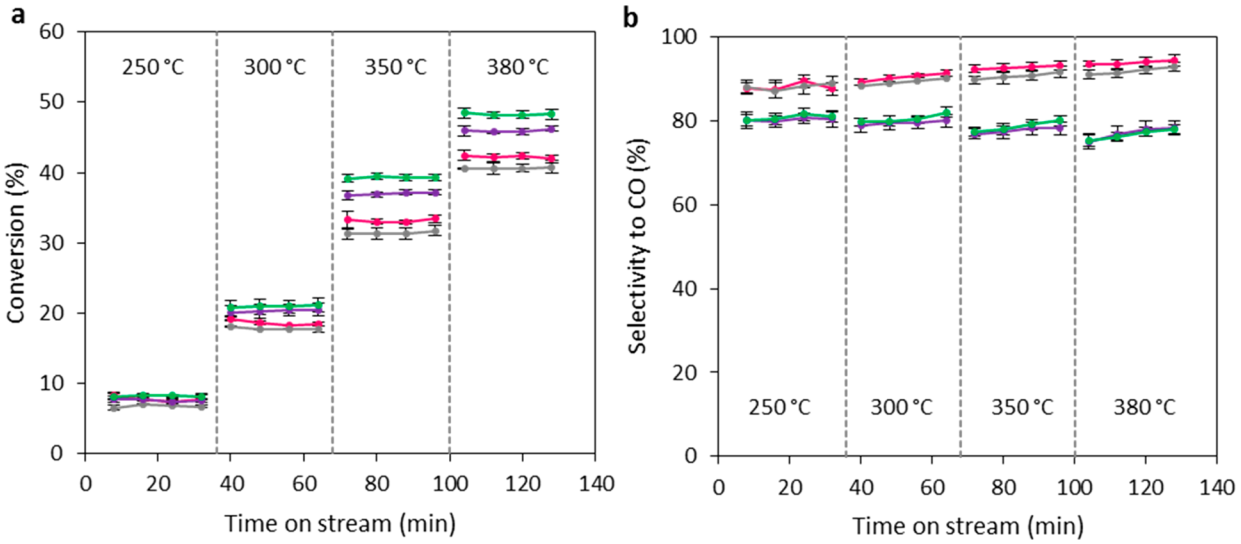

Figure 4. CO_2 reduction using PA treated 5%Pt/TiO_2 with NH_2 group in varying positions on tail. (a) CO_2 conversion and (b) CO selectivity with time on stream at different temperatures. Pink: 1-NH_2EPA/5%Pt/TiO_2; gray: 1-NH_2-2-M-PPA/5%Pt/TiO_2; purple: 2-NH_2EPA/5%Pt/TiO_2; green: 3-NH_2PPA/5%Pt/TiO_2. Catalyst loadings were kept at 80 mg for each case. Error bars indicate s.d. of triplicate runs. 1-NH_2EPA, (S)-(+)-1-aminoethylphosphonic acid; 1-NH_2-2-M-PPA, (1R)-(+)-(1-amino-2-methylpropyl)phosphonic acid; 2-NH_2EPA, 2-aminoethylphosphonic acid; 3-NH_2PPA, 3-aminopropylphosphonic aid.

However, the use of NH_2MPA for the modification retained the conversion in the low temperature range, although slightly lower conversion was still observed from 350 to 380 °C. The boost of activity upon introduction of the amine group agrees well with the enhanced CO_2 adsorption for amine-containing, PA-modified catalysts (Figure 1c and Figure S6). At higher temperatures, CO yield for NH_2MPA/5%Pt/TiO_2 was approaching thermodynamic equilibrium values due to the prevention of CO hydrogenation into CH_4,[15,48] which led to its lower conversion than 5%Pt/TiO_2.

To test the generality of the modification approach, we used the NH_2MPA to modify a different metal, Pd. The resultant NH_2MPA/5%Pd/TiO_2 showed far lower rates for CO_2 conversion (Figure 2c) although a large increase in CO selectivity was again observed (Figure 2d). The decreased activity was likely due to the fact that unlike Pt, the more oxophilic Pd can directly bond to PA ligands thereby suffering site blocking.[40] To address this issue, we used a "reverse deposition" procedure where PA was first deposited onto oxide supports followed by introducing metal through impregnation (Figure 3). Similar FTIR spectra were observed between the "reverse" and normal deposition (Figure S9), suggesting the formation of organic monolayers in a similar fashion. Moreover, the "reverse deposition" had a minimal effect on metal dispersion, as similar metal particle size was observed between the "reverse" and normal deposition (Figure S10 and Table S6). Using this strategy, the "reverse-deposited" Pd (5% Pd@NH_2MPA/TiO_2) largely restored CO_2 conversion rates of the unmodified 5%Pd/TiO_2 while significantly increasing the CO selectivity up to 99%. Figure S11 showed that after the modification with NH_2MPA, the CO production rates at 380 °C were enhanced by ~50% and ~400% for 5%Pt/TiO_2 and 5%Pd/TiO_2, respectively.

The effect of the amine group's position in PAs on CO_2 reduction was then investigated. The 5%Pt/TiO_2 was modified by different amine-containing PAs where the amine group was located on the α, β, or γ carbon. Figure 4b shows that the variations of the amine's position caused selectivity changes, as amine substitution at the α carbon exhibited CO selectivity around 90% while catalysts modified with the amine at β or γ carbon on PA showed CO selectivity around 80%. The observed selectivity is consistent with the corresponding CO desorption temperatures on these catalysts, as 2-NH_2EPA/5% Pt/TiO_2 showed a complete CO desorption temperature of

https://dx.doi.org/10.1021/jacs.9b12980
J. Am. Chem. Soc. 2020, 142, 5184−5193

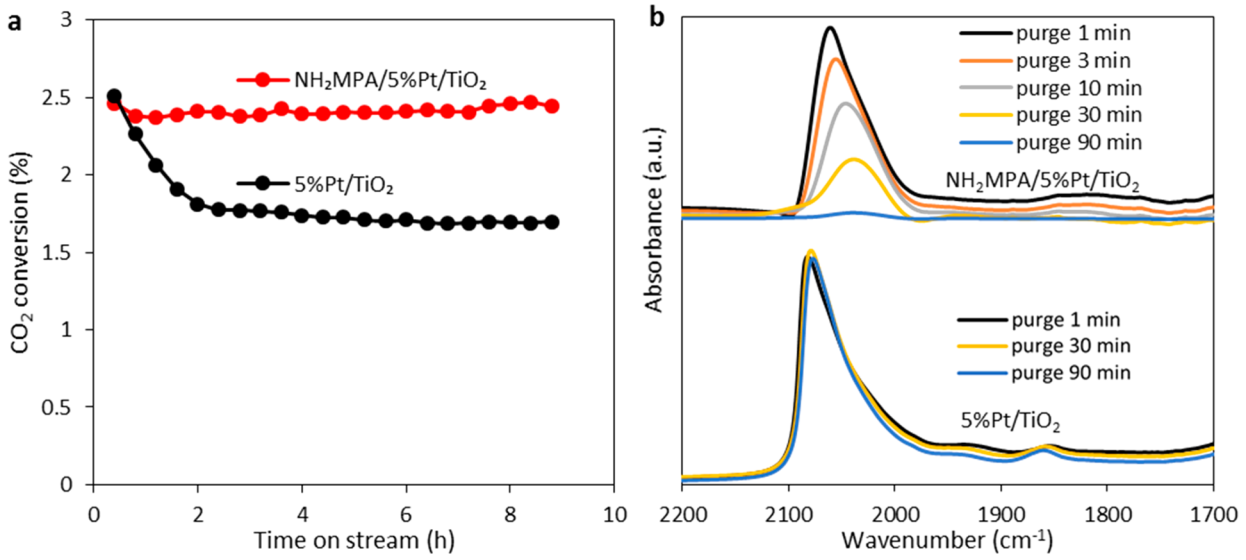

Figure 5. (a) Stability test during CO_2 reduction over modified and unmodified $5\%Pt/TiO_2$ catalysts under H_2 lean conditions. (b) *In situ* DRIFTS for modified versus unmodified $5\%Pt/TiO_2$ after 9 h of CO_2 reduction followed by purging. Reaction conditions: temperature, 250 °C; pressure, 1 atm; gas flow rates for CO_2 and H_2 are 5.6 and 1.4 mL min^{-1}, respectively; catalyst loadings were kept at 50 mg; the purge was performed at 250 °C under 100 mL min^{-1} Ar.

300 °C (Figure S12), higher than that for the α-carbon substituted amine containing PA but lower than the unmodified catalyst (Figure 1b). It is speculated that the position of the amine on PA may slightly affect the electronic properties of the interfacial active sites, thereby influencing their affinity to CO. DFT results for CO binding with MPA, 1-NH_2MPA, 1-NH_2EPA, and 2-NH_2EPA show that the α-substituted PAs, in fact, perturb the electronic properties of interfacial Pd active sites to a greater extent than the β-substituted PAs, leading to a 0.20 eV lower CO binding energy than for β substituted PAs (Table S10). Figure 4a shows that all amine-containing PAs promoted CO_2 conversion in a similar degree compared with PAs without the amine (Figure 2a) at a temperature range of 250−300 °C where the CO yield is well below the thermodynamic equilibrium values. The boost in activity is attributed to the fact that the CO_2 adsorption can also be promoted by non-α amines on the modified catalysts (Figure S6). Previous studies of carboxylic acid-functionalized PAs have shown that a secondary functional group in the PA tails can bend toward the surface-bound PA headgroup through intramolecular hydrogen-bonding interactions.[49] In the current study, the amine at the β or γ carbon may bend in a similar fashion to be still adjacent to the interface, thereby retaining the promotion effect of interfacial CO_2 adsorption.

Metal-catalyzed, low-temperature RWGS is susceptible to CO poisoning, resulting in partial catalyst deactivation.[50] To evaluate the catalyst stability, we performed CO_2 reduction over 9 h under H_2 lean conditions at 250 °C using both unmodified and NH_2MPA-modified $5\%Pt/TiO_2$. As shown in Figure 5a, the initial activity of the modified catalyst was retained during the entire course of reaction while apparent deactivation was observed for the unmodified catalyst, as its conversion dropped by ∼30% within the first 2 h of reaction. The minimal deactivation for the modified catalyst was presumably due to its weaker bonding to CO as indicated by its lower CO desorption temperature (Figure 1b and Figure S4). To validate this assumption, we performed *in situ* DRIFTS after the CO_2 reduction. Figure 5b shows that the CO adsorbed on modified catalyst could be completely removed after a purge with Ar at 250 °C while the CO on the unmodified catalyst remained adsorbed. The facile desorption of CO from the modified catalyst at the reaction conditions probably prevented the CO poisoning caused by strong CO-metal binding. Therefore, the current approach provided a means of not only achieving high selectivity and activity but also high poisoning resistance.

Extension to Other Metals and Supports. We used the same approach to modify another commonly used support, Al_2O_3, and found that the C−H stretching signals of $NH_2MPA/5\%Pt/Al_2O_3$ (Figure S13a) were similar to the ones of $NH_2MPA/5\%Pt/TiO_2$ (Figure 1a), indicating the formation of similar organic monolayers on Al_2O_3. The $NH_2MPA/5\%Pt/Al_2O_3$ enhanced CO selectivity up to 92% compared with a selectivity of ∼70% obtained by unmodified $5\%Pt/Al_2O_3$ at an equivalent conversion around 38% (Figure S13b,c). The modified catalyst also enhanced CO production rates (Figure S13d).

We also applied this approach to other metals. Figure 2c and Figure S11 showed a CO selectivity boost from 14% to 99% and a 5-fold CO production rate improvement at high CO_2 conversions after using NH_2MPA to modify $5\%Pd/TiO_2$, where "reverse deposition" was required to prevent PA blocking the Pd sites. We used both the normal and reverse deposition methods to modify $5\%Ni/Al_2O_3$ and found a similar trend: direct deposition of NH_2MPA onto the $5\%Ni/Al_2O_3$ improved CO selectivity from 7% to 73% but decreased CO_2 conversion rates by 1 order of magnitude, suggesting blocking of Ni sites by the modifier. In contrast, "reverse deposition" retained the activity of $5\%Ni/Al_2O_3$ while also increasing CO selectivity by a factor of 4 (Figure S14). It should be noted that the modified Ni catalyst showed lower selectivity to CO compared to those of the modified Pt or Pd catalysts, likely because Ni is more oxophilic than Pt and Pd, since the metal's oxophilicity can also strongly affect selectivity in CO_2 hydrogenation.[51]

https://dx.doi.org/10.1021/jacs.9b12980
J. Am. Chem. Soc. 2020, 142, 5184−5193

DISCUSSION

The key to using PAs to modify supported metal catalysts is to make use of the two "ends" of the organic ligands—the phosphonate head groups and the organic tail groups—to precisely tune interactions between catalyst and key reactive species. Here, this approach provided the opportunity to combine the through-surface effects of a conventional electronic modifier with the "through-space" effect of a stabilizing acid−base interaction in the near-surface environment.

The change of electronic properties leading to a partial positive charge on metal, which was presumably induced by the PA headgroup covalently bonding to catalyst support, is important for facile desorption of CO. In order to further validate the cause for the high selectivity, we modified the 5% Pt/TiO_2 by NH_2MPA using "reverse" deposition and then compared the catalytic results (Figure S15) with the one prepared by normal deposition (Figure 2a,b). We found almost identical degrees of selectivity improvement between the two at similar conversions ranging from 10% to 50%. The results further suggested that the PA deposition was primarily on the support but induced a change of the Pt electronic properties through the support to weaken the interaction of Pt with CO, as shown by the characterization results in Figure 1. We also increased the Pt particle size (from 3.9 to 9.8 nm) and observed a similar degree of selectivity promotion after its modification by PA (Figure S13e,f), suggesting that the enhancement of CO desorption by PA induced charge transfer seems to be relatively insensitive to Pt dispersion. Although a decreased equilibrium uptake of hydrogen was observed (Table S7), the PA modification did not appreciably affect hydrogen dissociation ability as similar H/D exchange rates during exposure to H_2/D_2 mixtures were observed before and after the modification (Table S8), possibly because the oxidation degree of the metal was not too strong to prevent H_2 dissociative adsorption. Since the PA modification weakens the metal's ability to coordinate CO while apparently not affecting hydrogenation, it could be used as a general strategy to construct anti-CO poisoning catalysts for hydrogenation reactions.[52,53]

In addition to the PA-headgroup induced change on the metal's electronic properties that facilitates CO desorption, the incorporation of amine groups within the PA tail can promote CO_2 adsorption to enhance reaction rates, as indicated by CO_2 DRIFTS results (Figure 1c and Figure S16b). Although a lower coverage of BZPA on $5\%Pt/TiO_2$, as compared to the one of $MPA/5\%Pt/TiO_2$ (Figure S1), may contribute to the higher CO_2 conversion rates of the former, $NH_2MPA/5\%Pt/TiO_2$ showed much higher rates than $BZPA/5\%Pt/TiO_2$ despite their similar PA coverage, which further supports the proposed promotion effect of the amine group. Furthermore, we performed kinetic studies (Figure S16a) and found a lower reaction order in CO_2 for NH_2MPA modified $5\%Pt/TiO_2$, compared with the ones modified with nonamine containing PAs, such as MPA and BZPA. The lower reaction order typically suggests stronger interaction between CO_2 and the catalytic surface.[54] In a comparison of the CO_2 reaction orders between $NH_2MPA/5\%Pt/TiO_2$ and $5\%Pt/TiO_2$, similar values were observed, suggesting that the amine group in PA strengthened the interaction with CO_2 to a level similar to that of the unmodified catalyst. We also observed a lower apparent activation energy for CO production after the $5\%Pt/TiO_2$ was modified by NH_2MPA (Figure S17).

It is useful to compare the acid−base interactions in the PAs for the use of basic metal oxides as supports. It has been reported that the use of strongly basic oxides such as MgO and CaO as catalysts can improve CO_2 adsorption and conversion, but can also cause strong adsorption of CO_2 as a surface carbonate species that is susceptible for deeper hydrogenation.[44,55−58] The higher CO production rates for NH_2MPA-modified catalysts indicate that the amine group led CO_2 to bond to the catalytic surface with a proper strength that would not cause excessively strong adsorption.[59,60]

In summary, we developed a method of using organophosphonic acid monolayers to modify supported metal catalysts for CO_2 reduction, with which a selectivity switch from methanation to RWGS was achieved. The dramatic change in catalytic performance originated from the collective effects of the head and tail groups on the ligands, which facilitated both CO_2 adsorption and CO desorption. With control of the ligands' molecular structure, CO_2 adsorption can be promoted through its interaction with the basic amine group on the ligands' tail; facile desorption of CO can be achieved by a change on the metal's electronic properties induced by the ligands' head groups binding to the support. After the modification, the selectivity toward CO was improved up to ∼99% without compromising the overall rates of CO_2 conversion, which translated to significantly enhanced CO production rates. Furthermore, deactivation was reduced for the modified catalyst due to the prevention of CO poisoning on the metal. The current study reveals a new avenue for using the versatility of the organic ligands to precisely tune the bonding strengths of multiple reactive species on a catalytic surface, thereby transforming nonselective catalysts into chemoselective metal catalysts for highly efficient RWGS.

METHODS

Catalyst Synthesis. Supported metal catalysts were prepared by the incipient wetness impregnation of metal onto each support. The metal precursors used were chloroplatinic acid hexahydrate, palladium dichloride, and nickel nitrate hexahydrate. The supports used were titanium oxide (P25) and γ-alumina. The prepared catalysts were reduced at 250 °C (for platinum and palladium) or 400 °C (for nickel) prior to use. The deposition of phosphonic acids was performed via the following steps. (1) The acid was dissolved in water (for PAs containing amine group) or tetrahydrofuran (for PAs without amine group) solution to make a 10 mM solution. Then, a corresponding amount of catalyst was added to the solution with stirring. The catalyst loading was controlled to ensure that the amount of acid in the solution was around ten times the amount of acid required to form a monolayer on the catalyst support. (2) Stirring was maintained for 16 h. (3) The resultant solid was then separated from the solution by centrifugation and annealed at 120 °C for 6 h in air. (4) The annealed material was washed with water or tetrahydrofuran five times followed by being dried at room temperature. During each wash, the material was mixed with copious amounts of water or tetrahydrofuran followed by centrifugation separation. The chemical structures of the phosphonic acids used in the current study are shown in Table S9.

Material Characterization. FTIR spectra were recorded using a Thermo Fisher Scientific Nicolet 6700 FTIR (100 scans at a resolution of 4 cm^{-1}). Carbon monoxide and carbon dioxide DRIFTS experiments were performed on the same FTIR equipped with a Harrick reaction chamber. XPS was performed using a Kratos AXIS Ultra DLD XPS system with a hemispherical energy analyzer and a monochromatic Al Kα source. XAS measurements were performed at

https://dx.doi.org/10.1021/jacs.9b12980
J. Am. Chem. Soc. 2020, 142, 5184−5193

the Brookhaven National Laboratory using beamline X18B at the National Synchrotron Light Source (NSLS). Elemental analysis was performed using inductively coupled plasma mass spectrometry. Transmission electron microscopy (TEM) images were obtained using a FEI Tecnai G2 20 Twin 200 kV LaB6 TEM (FEI, Hilsboro, OR) at an accelerating voltage of 200 kV. The dispersion of platinum was characterized by the chemisorption of hydrogen on a Micromeritics ChemiSorb 2720 system. H/D exchange experiment was performed using a tubular packed bed flow reactor at atmospheric pressure, the effluence of which was analyzed online by a mass spectrometry. Temperature-programmed reduction (60%H_2/He) was performed for PA modified catalysts, and an online mass spectrometry was used for effluent analysis during the temperature ramping. Details of the characterization methods are given in the Supporting Information.

Catalytic Reactions. Catalyst performance was evaluated in a tubular packed bed flow reactor at atmospheric pressure. Helium was mixed with hydrogen and carbon dioxide before reaching the catalyst bed. The reaction conditions (unless otherwise mentioned) were: temperature, 250−380 °C; pressure, 1 atm; gas flow rates for carbon dioxide and hydrogenation, 1.4 and 20 mL min^{-1}, respectively. Selectivities were calculated by dividing the conversion to one product by the total conversion. The reactor effluent was analyzed online using an SRI Instruments 8610C gas chromatograph equipped with a a Hayesep D column and a thermal conductivity detector. *In situ* DRIFTS was performed under the same reaction conditions as the gas-phase reactor. The FTIR spectra of fresh catalyst were used as background. Therefore, the collected signal displayed surface species during the reaction. For the catalyst stability test during CO_2 reduction, the reaction was performed under H_2 lean conditions. Experimental details are given in the Supporting Information.

■ ASSOCIATED CONTENT

Supporting Information

The Supporting Information is available free of charge at https://pubs.acs.org/doi/10.1021/jacs.9b12980.

Details of materials and synthesis; characterization including ICP, FTIR, DRIFTS, XPS, TPD, TEM, Chemisorption, H/D exchange rates; additional CO_2 hydrogenation results; computational methods and DFT results (PDF)

■ AUTHOR INFORMATION

Corresponding Author

J. Will Medlin − *Department of Chemical and Biological Engineering, University of Colorado, Boulder, Colorado 80309, United States;* orcid.org/0000-0003-2404-2443; Email: will.medlin@colorado.edu

Authors

Jing Zhang − *Department of Chemical and Biological Engineering, University of Colorado, Boulder, Colorado 80309, United States;* orcid.org/0000-0002-8213-4314

Shyam Deo − *Department of Chemical Engineering, The Pennsylvania State University, University Park, Pennsylvania 16802, United States*

Michael J. Janik − *Department of Chemical Engineering, The Pennsylvania State University, University Park, Pennsylvania 16802, United States;* orcid.org/0000-0001-9975-0650

Complete contact information is available at: https://pubs.acs.org/10.1021/jacs.9b12980

Notes

The authors declare no competing financial interest.

■ ACKNOWLEDGMENTS

This work was supported by the Department of Energy, Office of Science, Basic Energy Sciences Program, Chemical Sciences, Geosciences, and Biosciences Division [Grant No. DESC0005239]. We are also thankful to Dr. Lucas D. Ellis, Prof. Hans H Funke, Ryan Trottier, Alexander Jenkins, Caroline Frischmon (University of Colorado Boulder), Prof. Xinggui Zhou, Prof. Xuezhi Duan, Yao Shi, Yanqiang Tang (East China University of Science and Technology), and Nebojsa Marinkovic (Brookhaven National Laboratory) for their help in material characterizations and useful discussions.

■ REFERENCES

(1) Schlögl, R. Heterogeneous Catalysis. *Angew. Chem., Int. Ed.* **2015**, *54*, 3465−3520.

(2) Nielsen, D. U.; Hu, X. M.; Daasbjerg, K.; Skrydstrup, T. Chemically and Electrochemically Catalysed Conversion of CO_2 to CO with Follow-up Utilization to Value-Added Chemicals. *Nat. Catal.* **2018**, *1*, 244−254.

(3) Porosoff, M. D.; Yan, B.; Chen, J. G. Catalytic Reduction of CO_2 by H_2 for Synthesis of CO, Methanol and Hydrocarbons: Challenges and Opportunities. *Energy Environ. Sci.* **2016**, *9*, 62−73.

(4) Gao, P.; Li, S.; Bu, X.; Dang, S.; Liu, Z.; Wang, H.; Zhong, L.; Qiu, M.; Yang, C.; Cai, J.; Wei, W.; Sun, Y. Direct Conversion of CO_2 into Liquid Fuels with High Selectivity over a Bifunctional Catalyst. *Nat. Chem.* **2017**, *9*, 1019−1024.

(5) Qian, C.; Sun, W.; Hung, D. L. H.; Qiu, C.; Makaremi, M.; Hari Kumar, S. G.; Wan, L.; Ghoussoub, M.; Wood, T. E.; Xia, M.; Tountas, A.; Li, Y.; Dong, Y.; Gourevich, I.; Singh, C.; Ozin, G. Catalytic CO_2 Reduction by Palladium-Decorated Silicon−Hydride Nanosheets. *Nat. Catal.* **2019**, *2*, 46−54.

(6) Kattel, S.; Yu, W.; Yang, X.; Yan, B.; Huang, Y.; Wan, W.; Liu, P.; Chen, J. G. CO_2 Hydrogenation over Oxide-Supported PtCo Catalysts: The Role of the Oxide Support in Determining the Product Selectivity. *Angew. Chem., Int. Ed.* **2016**, *55*, 7968−7973.

(7) Wei, J.; Ge, Q.; Yao, R.; Wen, Z.; Fang, C.; Guo, L.; Xu, H.; Sun, J. Directly Converting CO_2 into a Gasoline Fuel. *Nat. Commun.* **2017**, *8*, 15174.

(8) Kattel, S.; Yan, B.; Yang, Y.; Chen, J. G.; Liu, P. Optimizing Binding Energies of Key Intermediates for CO_2 Hydrogenation to Methanol over Oxide-Supported Copper. *J. Am. Chem. Soc.* **2016**, *138*, 12440−12450.

(9) Tang, Q.-L.; Hong, Q.-J.; Liu, Z.-P. CO_2 Fixation into Methanol at Cu/ZrO_2 Interface from First Principles Kinetic Monte Carlo. *J. Catal.* **2009**, *263*, 114−122.

(10) Kattel, S.; Yan, B.; Chen, J. G.; Liu, P. CO_2 Hydrogenation on Pt, Pt/SiO_2 and Pt/TiO_2: Importance of Synergy between Pt and Oxide Support. *J. Catal.* **2016**, *343*, 115−126.

(11) Kattel, S.; Liu, P.; Chen, J. G. Tuning Selectivity of CO_2 Hydrogenation Reactions at the Metal/Oxide Interface. *J. Am. Chem. Soc.* **2017**, *139*, 9739−9754.

(12) Porosoff, M. D.; Baldwin, J. W.; Peng, X.; Mpourmpakis, G.; Willauer, H. D. Potassium-Promoted Molybdenum Carbide as a Highly Active and Selective Catalyst for CO_2 Conversion to CO. *ChemSusChem* **2017**, *10*, 2408−2415.

(13) Joo, O. S.; Jung, K. D.; Moon, I.; Rozovskii, A. Y.; Lin, G. I.; Han, S. H.; Uhm, S. J. Carbon Dioxide Hydrogenation to Form Methanol via a Reverse-Water-Gas- Shift Reaction (the CAMERE Process). *Ind. Eng. Chem. Res.* **1999**, *38*, 1808−1812.

(14) Park, S. W.; Joo, O. S.; Jung, K. D.; Kim, H.; Han, S. H. ZnO/Cr2O3 Catalyst for Reverse-Water-Gas-Shift Reaction of CAMERE Process. *Korean J. Chem. Eng.* **2000**, *17*, 719−722.

(15) Winter, L. R.; Gomez, E.; Yan, B.; Yao, S.; Chen, J. G. Tuning Ni-Catalyzed CO_2 Hydrogenation Selectivity via Ni-Ceria Support Interactions and Ni-Fe Bimetallic Formation. *Appl. Catal., B* **2018**, *224*, 442−450.

(16) Porosoff, M. D.; Chen, J. G. Trends in the Catalytic Reduction of CO_2 by Hydrogen over Supported Monometallic and Bimetallic Catalysts. *J. Catal.* **2013**, *301*, 30−37.
(17) Alayoglu, S.; Beaumont, S. K.; Zheng, F.; Pushkarev, V. V.; Zheng, H.; Iablokov, V.; Liu, Z.; Guo, J.; Kruse, N.; Somorjai, G. A. CO_2 Hydrogenation Studies on Co and CoPt Bimetallic Nanoparticles under Reaction Conditions Using TEM, XPS and NEXAFS. *Top. Catal.* **2011**, *54*, 778−785.
(18) Yin, G.; Yuan, X.; Du, X.; Zhao, W.; Bi, Q.; Huang, F. Efficient Reduction of CO_2 to CO Using Cobalt−Cobalt Oxide Core−Shell Catalysts. *Chem. - Eur. J.* **2018**, *24*, 2157−2163.
(19) Dou, J.; Sheng, Y.; Choong, C.; Chen, L.; Zeng, H. C. Silica Nanowires Encapsulated Ru Nanoparticles as Stable Nanocatalysts for Selective Hydrogenation of CO_2 to CO. *Appl. Catal., B* **2017**, *219*, 580−591.
(20) Luc, W.; Collins, C.; Wang, S.; Xin, H.; He, K.; Kang, Y.; Jiao, F. Ag-Sn Bimetallic Catalyst with a Core-Shell Structure for CO_2 Reduction. *J. Am. Chem. Soc.* **2017**, *139*, 1885−1893.
(21) Zhang, J.; Medlin, J. W. Catalyst Design Using an Inverse Strategy: From Mechanistic Studies on Inverted Model Catalysts to Applications of Oxide-Coated Metal Nanoparticles. *Surf. Sci. Rep.* **2018**, *73*, 117−152.
(22) Liu, Q.; Yang, X.; Li, L.; Miao, S.; Li, Y.; Li, Y.; Wang, X.; Huang, Y.; Zhang, T. Direct Catalytic Hydrogenation of CO_2 to Formate over a Schiff-Base-Mediated Gold Nanocatalyst. *Nat. Commun.* **2017**, *8*, 1407.
(23) Matsubu, J. C.; Zhang, S.; DeRita, L.; Marinkovic, N. S.; Chen, J. G.; Graham, G. W.; Pan, X.; Christopher, P. Adsorbate-Mediated Strong Metal-Support Interactions in Oxide-Supported Rh Catalysts. *Nat. Chem.* **2017**, *9*, 120−127.
(24) Vogt, C.; Groeneveld, E.; Kamsma, G.; Nachtegaal, M.; Lu, L.; Kiely, C. J.; Berben, P. H.; Meirer, F.; Weckhuysen, B. M. Unravelling Structure Sensitivity in CO_2 Hydrogenation over Nickel. *Nat. Catal.* **2018**, *1*, 127−134.
(25) Gonçalves, R. V.; Vono, L. L. R.; Wojcieszak, R.; Dias, C. S. B.; Wender, H.; Teixeira-Neto, E.; Rossi, L. M. Selective Hydrogenation of CO_2 into CO on a Highly Dispersed Nickel Catalyst Obtained by Magnetron Sputtering Deposition: A Step towards Liquid Fuels. *Appl. Catal., B* **2017**, *209*, 240−246.
(26) Kwak, J. H.; Kovarik, L.; Szanyi, J. CO_2 Reduction on Supported Ru/Al_2O_3 Catalysts: Cluster Size Dependence of Product Selectivity. *ACS Catal.* **2013**, *3*, 2449−2455.
(27) Aitbekova, A.; Wu, L.; Wrasman, C. J.; Boubnov, A.; Hoffman, A. S.; Goodman, E. D.; Bare, S. R.; Cargnello, M. Low-Temperature Restructuring of CeO_2-Supported Ru Nanoparticles Determines Selectivity in CO_2 Catalytic Reduction. *J. Am. Chem. Soc.* **2018**, *140*, 13736−13745.
(28) Matsubu, J. C.; Yang, V. N.; Christopher, P. Isolated Metal Active Site Concentration and Stability Control Catalytic CO_2 reduction Selectivity. *J. Am. Chem. Soc.* **2015**, *137*, 3076−3084.
(29) Schoenbaum, C. A.; Schwartz, D. K.; Medlin, J. W. Controlling the Surface Environment of Heterogeneous Catalysts Using Self-Assembled Monolayers. *Acc. Chem. Res.* **2014**, *47*, 1438−1445.
(30) Marshall, S. T.; O'Brien, M.; Oetter, B.; Corpuz, A.; Richards, R. M.; Schwartz, D. K.; Medlin, J. W. Controlled Selectivity for Palladium Catalysts Using Self-Assembled Monolayers. *Nat. Mater.* **2010**, *9*, 853−858.
(31) Hostetler, M. J.; Stokes, J. J.; Murray, R. W. Infrared Spectroscopy of Three-Dimensional Self-Assembled Monolayers: A N-Alkanethiolate Monolayers on Gold Cluster Compounds. *Langmuir* **1996**, *12*, 3604−3612.
(32) Hadjiivanov, K. Identification and Characterization of Surface Hydroxyl Groups by Infrared Spectroscopy. *Adv. Catal.* **2014**, *57*, 99−318.
(33) Hauffman, T.; Blajiev, O.; Snauwaert, J.; van Haesendonck, C.; Hubin, A.; Terryn, H. Study of the Self-Assembling of n -Octylphosphonic Acid Layers on Aluminum Oxide. *Langmuir* **2008**, *24*, 13450−13456.
(34) Hoque, E.; Derose, J. A.; Kulik, G.; Hoffmann, P.; Mathieu, H. J.; Bhushan, B. Alkylphosphonate Modified Aluminum Oxide Surfaces. *J. Phys. Chem. B* **2006**, *110*, 10855−10861.
(35) Wilfong, W. C.; Srikanth, C. S.; Chuang, S. S. C. In Situ ATR and DRIFTS Studies of the Nature of Adsorbed CO_2 on Tetraethylenepentamine Films. *ACS Appl. Mater. Interfaces* **2014**, *6*, 13617−13626.
(36) Rodriguez, J. A.; Campbell, R. A.; Goodman, D. W. Electron Donor-Electron Acceptor Interactions in Bimetallic Surfaces: Theory and XPS Studies. *J. Phys. Chem.* **1991**, *95*, 5716−5719.
(37) Campbell, R. A.; Rodriguez, J. A.; Goodman, D. W. An X-Ray Photoelectron Spectroscopic Study of the Electronic Properties of Ultrathin Ni Films on Ru(0001) and Mo(110). *Surf. Sci.* **1991**, *256*, 272−280.
(38) Singh, J.; Alayon, E. M. C.; Tromp, M.; Safonova, O. V.; Glatzel, P.; Nachtegaal, M.; Frahm, R.; Van Bokhoven, J. A. Generating Highly Active Partially Oxidized Platinum during Oxidation of Carbon Monoxide over Pt/Al_2O_3: In Situ, Time-Resolved, and High-Energy-Resolution X-Ray Absorption Spectroscopy. *Angew. Chem., Int. Ed.* **2008**, *47*, 9260−9264.
(39) Rodriguez, J. A.; Goodman, D. W. The Nature of the Metal-Metal Bond in Bimetallic Surfaces. *Science* **1992**, *257*, 897−903.
(40) Zhang, J.; Ellis, L. D.; Wang, B.; Dzara, M. J.; Sievers, C.; Pylypenko, S.; Nikolla, E.; Medlin, J. W. Control of Interfacial Acid−Metal Catalysis with Organic Monolayers. *Nat. Catal.* **2018**, *1*, 148−155.
(41) Lambert, J. B.; Emblidge, R. W.; Zhao, Y. Participation of the β Phosphonate Group in Carbocation Formation. *J. Org. Chem.* **1994**, *59*, 5397−5403.
(42) Deo, S.; Medlin, W.; Nikolla, E.; Janik, M. J. Reaction Paths for Hydrodeoxygenation of Furfuryl Alcohol at TiO_2/Pd Interfaces. *J. Catal.* **2019**, *377*, 28−40.
(43) Brodard-Severac, F.; Guerrero, G.; Maquet, J.; Florian, P.; Gervais, C.; Mutin, P. H. High-Field 17 O MAS NMR Investigation of Phosphonic Acid Monolayers on Titania. *Chem. Mater.* **2008**, *20*, 5191−5196.
(44) Das, T.; Deo, G. Synthesis, Characterization and in Situ DRIFTS during the CO_2 hydrogenation Reaction over Supported Cobalt Catalysts. *J. Mol. Catal. A: Chem.* **2011**, *350*, 75−82.
(45) Wang, X.; Shi, H.; Kwak, J. H.; Szanyi, J. Mechanism of CO_2 Hydrogenation on Pd/Al_2O_3 Catalysts: Kinetics and Transient DRIFTS-MS Studies. *ACS Catal.* **2015**, *5*, 6337−6349.
(46) Peng, Y.; Wang, L.; Luo, Q.; Cao, Y.; Dai, Y.; Li, Z.; Li, H.; Zheng, X.; Yan, W.; Yang, J.; Zeng, J. Molecular-Level Insight into How Hydroxyl Groups Boost Catalytic Activity in CO_2 Hydrogenation into Methanol. *Chem.* **2018**, *4*, 613−625.
(47) Bacsik, Z.; Ahlsten, N.; Ziadi, A.; Zhao, G.; Garcia-Bennett, A. E.; Martín-Matute, B.; Hedin, N. Mechanisms and Kinetics for Sorption of CO_2 on Bicontinuous Mesoporous Silica Modified with N-Propylamine. *Langmuir* **2011**, *27*, 11118−11128.
(48) Riedel, T.; Schaub, G.; Jun, K.-W.; Lee, K.-W. Kinetics of CO_2 Hydrogenation on a K-Promoted Fe Catalyst. *Ind. Eng. Chem. Res.* **2001**, *40*, 1355−1363.
(49) Coan, P. D.; Ellis, L. D.; Griffin, M. B.; Schwartz, D. K.; Medlin, J. W. Enhancing Cooperativity in Bifunctional Acid-Pd Catalysts with Carboxylic Acid-Functionalized Organic Monolayers. *J. Phys. Chem. C* **2018**, *122*, 6637−6647.
(50) Goguet, A.; Meunier, F.; Breen, J. P.; Burch, R.; Petch, M. I.; Faur Ghenciu, A. Study of the Origin of the Deactivation of a Pt/CeO_2 Catalyst during Reverse Water Gas Shift (RWGS) Reaction. *J. Catal.* **2004**, *226*, 382−392.
(51) Avanesian, T.; Gusmão, G. S.; Christopher, P. Mechanism of CO_2 Reduction by H_2 on Ru(0 0 0 1) and General Selectivity Descriptors for Late-Transition Metal Catalysts. *J. Catal.* **2016**, *343*, 86−96.
(52) Liu, J.; Lucci, F. R.; Yang, M.; Lee, S.; Marcinkowski, M. D.; Therrien, A. J.; Williams, C. T.; Sykes, E. C. H.; Flytzani-Stephanopoulos, M. Tackling CO Poisoning with Single-Atom Alloy Catalysts. *J. Am. Chem. Soc.* **2016**, *138*, 6396−6399.

https://dx.doi.org/10.1021/jacs.9b12980
J. Am. Chem. Soc. 2020, 142, 5184−5193

(53) Giannakakis, G.; Flytzani-Stephanopoulos, M.; Sykes, E. C. H. Single-Atom Alloys as a Reductionist Approach to the Rational Design of Heterogeneous Catalysts. *Acc. Chem. Res.* **2019**, *52*, 237−247.
(54) Weatherbee, G. D.; Bartholomew, C. H. Hydrogenation of CO_2 on Group VIII Metals. II. Kinetics and Mechanism of CO_2 Hydrogenation on Nickel. *J. Catal.* **1982**, *77*, 460−472.
(55) Park, J. N.; McFarland, E. W. A Highly Dispersed Pd-Mg/SiO_2 Catalyst Active for Methanation of CO_2. *J. Catal.* **2009**, *266*, 92−97.
(56) Aldana, P. A. U.; Ocampo, F.; Kobl, K.; Louis, B.; Thibault-Starzyk, F.; Daturi, M.; Bazin, P.; Thomas, S.; Roger, A. C. Catalytic CO_2 Valorization into CH_4 on Ni-Based Ceria-Zirconia. Reaction Mechanism by Operando IR Spectroscopy. *Catal. Today* **2013**, *215*, 201−207.
(57) Duyar, M. S.; Treviño, M. A. A.; Farrauto, R. J. Dual Function Materials for CO_2 Capture and Conversion Using Renewable H_2. *Appl. Catal., B* **2015**, *168*−*169*, 370−376.
(58) Niu, J.; Liland, S. E.; Yang, J.; Rout, K. R.; Ran, J.; Chen, D. Effect of Oxide Additives on the Hydrotalcite Derived Ni Catalysts for CO_2 Reforming of Methane. *Chem. Eng. J.* **2019**, *377*, 119763.
(59) Didas, S. A.; Choi, S.; Chaikittisilp, W.; Jones, C. W. Amine-Oxide Hybrid Materials for CO_2 Capture from Ambient Air. *Acc. Chem. Res.* **2015**, *48*, 2680−2687.
(60) Alesi, W. R.; Gray, M.; Kitchin, J. R. CO_2 Adsorption on Supported Molecular Amidine Systems on Activated Carbon. *ChemSusChem* **2010**, *3*, 948−956.

https://dx.doi.org/10.1021/jacs.9b12980
J. Am. Chem. Soc. 2020, 142, 5184−5193